Supporting Information

Atomically Precise Arrays of Fluorescent Silver Clusters: A Modular Approach for Metal Cluster Photonics on DNA Nanostructures

Stacy M. Copp[†], Danielle E. Schultz[‡], Steven Swasey[‡], & Elisabeth G. Gwinn*,[†]

[†] Department of Physics, University of California – Santa Barbara, Santa Barbara, CA, USA
[‡] Department of Chemistry, University of California – Santa Barbara, Santa Barbara, CA, USA

*Corresponding author: e-mail: bgwinn@physics.ucsb.edu

Table of Contents

I. DNA sequences (Table S1) ····· 2

II. Attachment of Cy5 to NT *via* AT-rich tail (Fig.S1) ····· 3

III. Selection of Ag_{15}-DNA host strand (Fig. S2) ····· 4

IV. Selection of Ag_{14}-DNA host strand (Fig. S3) ····· 5

V. Purification of Ag_{15}-DNA and Ag_{14}-DNA emitters ····· 6

VI. Microscopy of NT with docker sites (Fig. S4, S5) ····· 8

VII. NT contour intensity mapping and simulations (Fig. S6, S7) ····· 9

VIII. Ag_{14}-DNA-decorated NT microscopy (Fig. S8) ····· 11

IX. Individual Ag_{15}-DNA blinking on NT with 10% docker sites (Fig. S9, Movie S1) ····· 12

X. Comparing *M* values for NT labeled with once- and twice-purified Ag_{15}-DNA ····· 13

XI. References ····· 14

I. DNA sequences

Name	Sequence (5' – 3')
U1	GGCGATTAGG-ACGCTAAGCCA-CCTTTAGATCC-TGTATCTGGT
U2	GGATCTAAAGG-ACCAGATACA-CCACTCTTCC-TGACATCTTGT
U3	GGAAGAGTGG-ACAAGATGTCA-CCGTGAGAACC-TGCAATGCGT
U4	GGTTCTCACGG-ACGCATTGCA-CCGCACGACC-TGTTCGACAGT
U5	GGTCGTGCGG-ACTGTCGAACA-CCAACGATGCC-TGATAGAAGT
U6	GGCATCGTTGG-ACTTCTATCA-ATGCACCTCC-AGCTTTGAATG
U7	GGAGGTGCAT-CATTCAAAGCT-AACGGTAACTA-TGACTTGGGA
U8	TAGTTACCGTT-TCCCAAGTCA-AACACTAGAC-ACATGCTCCTA
U9	GTCTAGTGTT-TAGGAGCATGT-CGAGACTACAC-CCTTGCCACC
T10	GTGTAGTCTCG-GGTGGCAAGG-CCTAATCGCC-TGGCTTAGCGT
U6-docker	GGCATCGTTGG-ACTTCTATCA-ATGCACCTCC-AGCTTTGAATG-TTTT-ATTTATACAACGGA
U9-docker	GTCTAGTGTT-TAGGAGCATGT-CGAGACTACAC-CCTTGCCACC-TTTT-ATTAACACAAGACA
Ag_{14}-DNA host, U9	TTCCCACCCACCCCGGCCCGTT-TTTT- TGTCTTGTGT
Ag_{15}-DNA host, U6	CACCGCTTTTGCCTTTTGGGGACGGATA-TTTT-TCCGTTGTATAAAT

Table S1: Sequences of DNA oligomers. 10-helix DNA nanotube (NT) construction oligomers (U1 – U9, T10),[1] modified NT oligomers with docking sites (U6-docker, U9-docker), and Ag_N-DNA host strands (template – TTTT – linker).

II. Attachment of Cy5 to NT *via* AT-rich tail

As described in the main text, AT-rich tails can prove unsuitable to use for attachment of decorating elements to DNA nanotubes (NT) due to the limited sequence space, which challenges choice of sequences without self-complementary . Here, a 30-base A,T tail developed elsewhere[2] was appended to the 3' end of U6, and its complement was labeled with Cy5 dye. Attachment of this Cy5-labeled oligomer to FAM-labeled nanotubes annealed with the modified U6 strand was only observable for a select few images – the image below is *not* a representative image but is a "*best case*" image showing colocalization of DNA nanotubes (green) with incomplete Cy5 labeling on a fraction of the nanotubes. Due to the AT-rich tail's high degree of self-complementarity, the strands often aggregate instead of labeling the nanotubes, and the nanotubes themselves also aggregate.

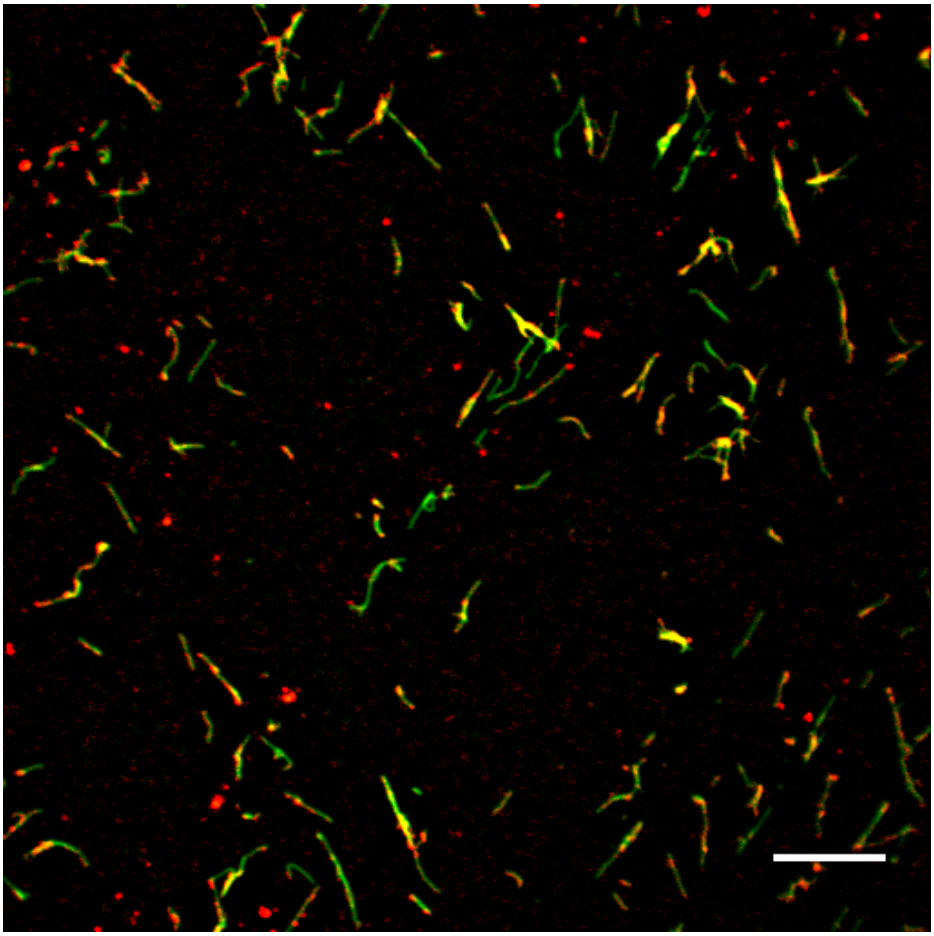

Figure S1: Confocal images of fluorescein (FAM) labeled NT with 100% U6 AT-rich docking sites, decorated with Cy5-labeled AT-rich complements after tube formation. Samples are in aqueous buffer on clean glass coverslips. Scale bar is 10 μm. Overlap of red (Cy5) and green (FAM) channels shows some colocalization, indicating that a fraction of the Cy-AT oligomers dock onto the nanotubes, while large red aggregates also form due to self-complementarity of the AT-rich tail.

III. Selection of Ag_{15}-DNA host strand

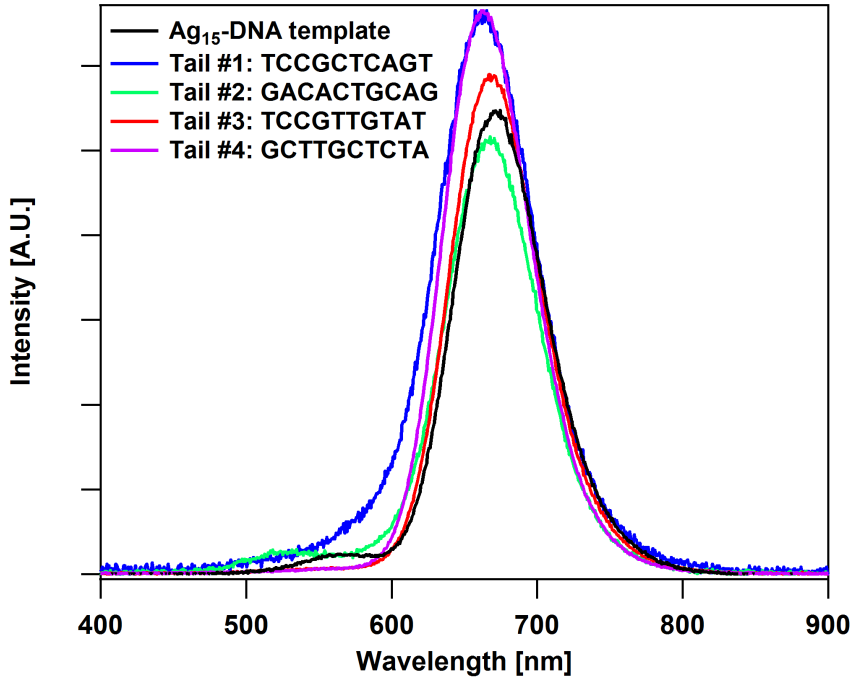

Figure S2: UV-excited fluorescence spectra of unpurified Ag_N-DNA stabilized by the template strand for Ag_{15}-DNA (black) and with appended candidate linker regions at the 3' end of that template (blue, green, red, magenta). All syntheses were performed with 15.0 μM DNA, 188 μM AgNO3, 93.8 μM NaBH4, and 10 mM NH4OAc (corresponding to 12.5 Ag atoms per host strand; Ag/base ratios vary with host strand length). Spectra are normalized to the absorbance peak corresponding to the dominant fluorescent product (~ 600 nm peak absorbance). Tail #3 was selected for a linker region because spectra of Ag_N-DNA stabilized by this template most closely resemble those stabilized by the Ag_{15}-DNA template alone, indicating highest yield of the desired cluster product. Subsequent purification isolates the Ag_{15}-DNA.

IV. Selection of Ag_{14}-DNA host strand

Host strands for Ag_{14}-DNA were selected using the same methods described for Ag_{15}-DNA in the main text. The Ag_{14}-DNA used here has peak fluorescence excitation and emission at ~570 nm and ~637 nm, respectively, and a 93% quantum yield. Its size and quantum yield were previously determined elsewhere.[3] This silver cluster is templated by the DNA oligomer TCCCACCCACCCCGGCCCGTT. To discover appropriate sequences for linking regions appended to the 3' end of this sequence, 6 candidate 10-base sequences previously found to be unfavorable for formation of fluorescent silver clusters[4,5] were appended to the 3' end of Ag_{14}-DNA's template sequence, separated by 4 thymines. Candidate host strands thus had the sequence: TCCCACCCACCCCGGCCCGTT-TTTT-'10 base oligomer'.

Emission spectra of Ag_N-DNA products formed on these candidate host strands were compared to the spectrum of Ag_{14}-DNA (Figure S3). The similarity of the spectra in Figure S3 strongly suggest that Ag_N-DNA formed by the modified host strands also contain N = 14 Ag atoms. Tail #5 was selected for HPLC purification because Ag_N-DNA stabilized by this template closely resemble those stabilized by the Ag_{14}-DNA template alone and because its complement has low complementarity with the oligomers composing the NT. The complement of Tail #5 was appended to the 3' end of the U9 oligomer.

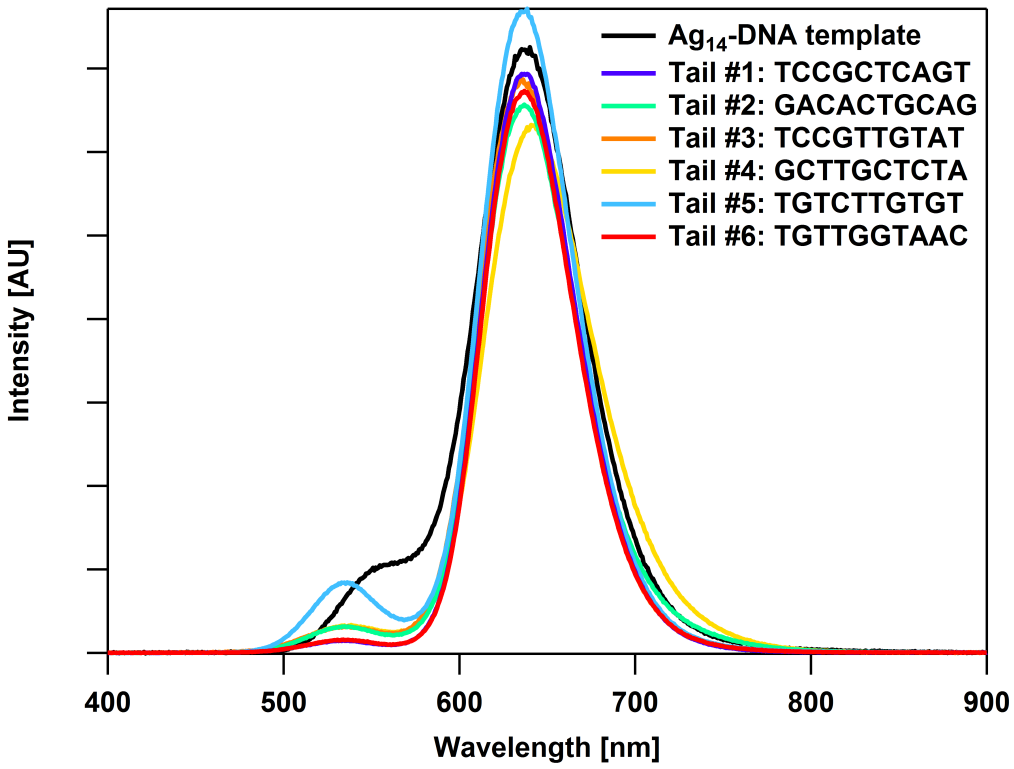

Figure S3: UV-excited fluorescence spectra of unpurified Ag_N-DNA stabilized by the template strand for Ag_{14}-DNA (black) and with appended candidate linker regions at the 3' end of that template. All syntheses were performed with 15.0 µM DNA, 188 µM AgNO3, 93.8 µM NaBH4, and 10 mM NH4OAc (corresponding to 12.5 Ag atoms per host strand; Ag/base ratios vary with host strand length). Spectra are normalized to the absorbance peak corresponding to the dominant fluorescent product (~ 570 nm peak absorbance).

V. Purification of Ag_{15}-DNA and Ag_{14}-DNA emitters

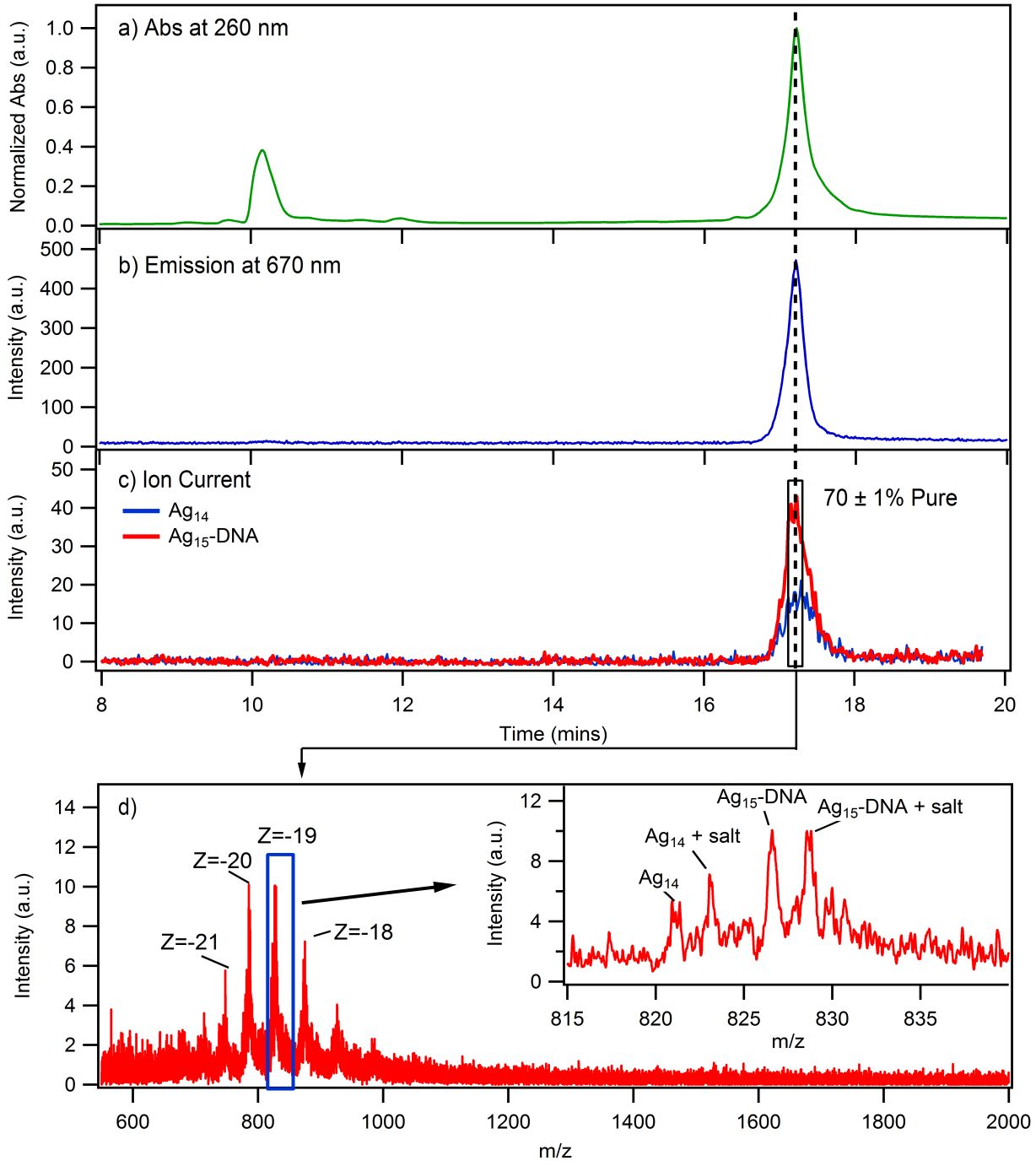

Figure S4: Second round HFIP purification chromatograms of Ag_{15}-DNA for a) absorbance at 260 nm, b) emission at 670 nm, the peak fluorescemce wavelength of the Ag_{15}-DNA in the running buffer; and c) the ion current of the major species in the elution window over which the sample for nanotube attachment was caught (black, boxed area). The 70 ± 1% purity estimate is based on the integrated ion current of Ag_{15}-DNA relative to all other silver species attached to DNA present in the catch window. The same window was used to compile the mass spectrum in (d), showing a range of major charge states (Z = -18 to -21) with the inset representing the blue, boxed area of the mass spectrum which displays all prominent species present at one charge state (Z = -19).

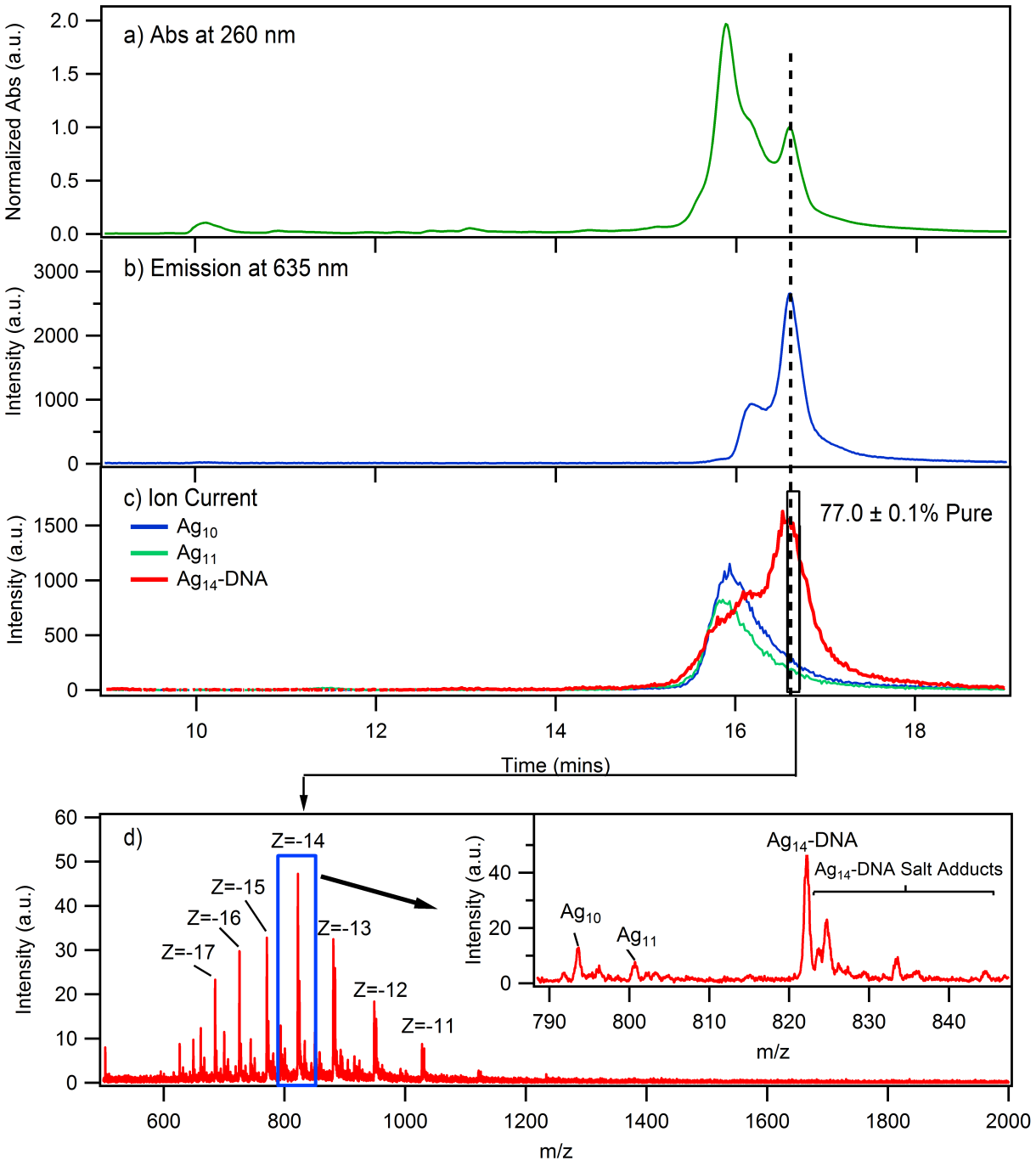

Figure S5: Second round HFIP purification chromatograms of Ag_{14}-DNA for a) absorbance at 260 nm, b) emission at Ag_{14}-DNA's fluorescence peak wavelength in running buffer, 635 nm; and c) the ion current of the major species in the window that the sample was caught (black, boxed area) for nanotube attachment. The 77.0 ± 0.1% purity estimate is based on the integrated ion current of Ag_{14}-DNA relative to all other silver species attached to DNA present in the catch window. The same window was used to compile the mass spectrum in (d), showing a range of major charge states (Z = -11 to -17) with the inset representing the blue, boxed area of the mass spectrum which displays all prominent species present at one charge state (Z = -14).

VI. Microscopy of NT with docker sites

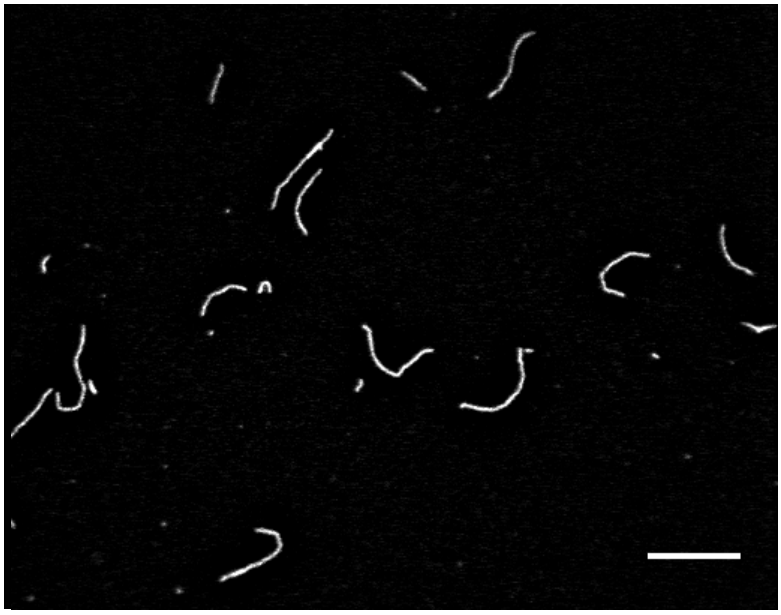

Figure S6: Spinning disc confocal image of fluorescein-labeled 10-helix DNA nanotubes[1] (NT) in a polyvinyl alcohol (PVA) film. Proper nanotube formation with an appended 14-base docker site on the 3' end of the 100% of the U6 NT oligomers is evident in this representative image. Scale bar: 10 μm.

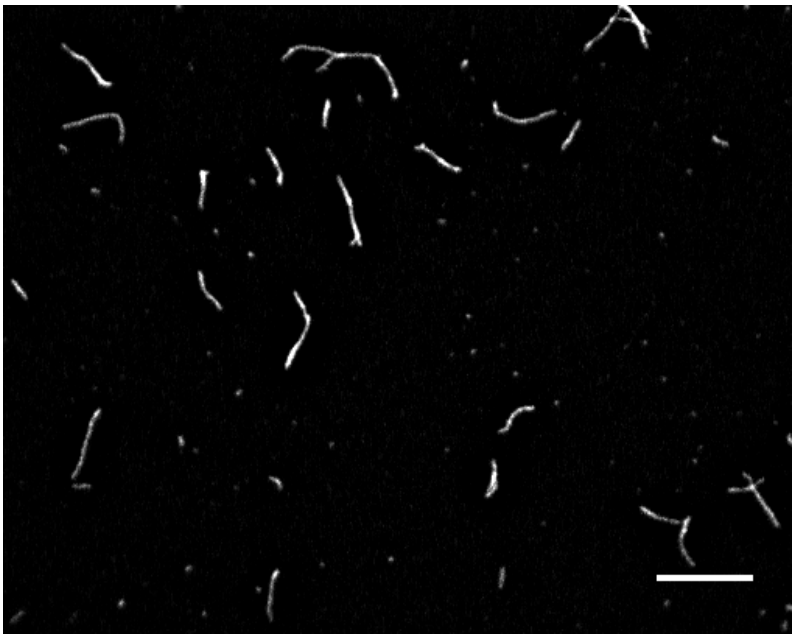

Figure S7: Spinning disc confocal image of fluorescein-labeled 10-helix DNA nanotubes[1] (NT) in a polyvinyl alcohol (PVA) film. Proper nanotube formation with an appended 14-base docker site on the 3' end of the 100% of the U9 NT oligomers is evident in this representative image, albeit with more defects visible than for NT with different docking sites appended to the U6 oligomers (Figure S4). Scale bar: 10 μm.

VII. NT contour intensity mapping and simulations

DNA nanotube (NT) contours were traced using a MATLAB script from the Paul Wiggins group at the University of Washington,[6] with 2 pixel step size between points along a single NT trace. The EMCCD camera used here for microscopy has a pixel size of 0.16 µm. To investigate intensity fluctuations along NT, the extracted NT contours are imported into a custom MATLAB script that calculates the peak intensity at each point along the NT contour, using 10-pixel cross-sections perpendicular to a NT contour trace and averaging intensity over a 5-pixel window centered on the NT. Local background correction is achieved by subtracting the average intensity of the ends of the cross-sections, which extend far from the NT contour (Figure S6). Then, the standard deviation of the intensity along the NT contour is calculated for each NT, normalized to the average intensity of all points along the NT contour, as a quantitative measure of intensity fluctuations along NT that is invariant to variations in intensity among different NT. The average of this standard deviation over the population of all tubes is called *M*.

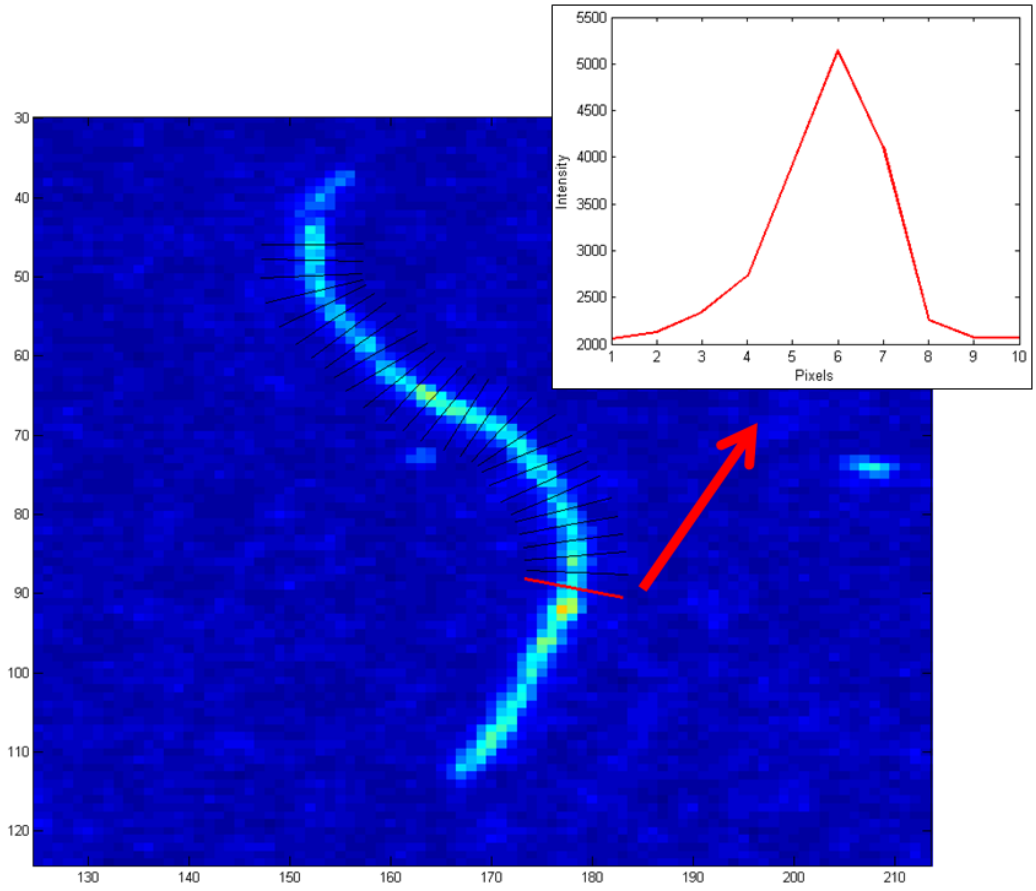

Figure S8: Example image of cross-sections on an Ag_{15}-DNA-labeled NT, with 100% U6 docking sites, as produced by the custom MATLAB script. The intensity profile of the red cross-section is plotted in the upper right. Local background correction is achieved by subtracting the average of the endpoints of this intensity profile, and the average intensity of the NT at this point along the NT contour is calculated by taking the 5-pixel-wide average of the intensity, centered at the maximum intensity of the intensity profile.

While *M* can act as a relative comparison of intensity fluctuations between different species of NT, it is necessary to perform simulations of NT with certain labeling percentages and emitter dipole orientations in order to understand what values of *M* might be expected for various labeling scenarios. Using MATLAB, we simulated microscope images of NT with decorating emitters randomly arranged on docking sites with 7.1 nm spacing, using the specifics of the microscope objective and camera used for microscopy, described in I. Experimental Methods, for various % labeling. For each point in Figure S7, 100 such simulated NT were used to calculate the average value and standard deviation of *M*. In the case of emitters with no dipolar dependence (yellow), that is, all emitters couple equally to the microscope objective, $M = 0$ for NT with 100% of docking sites labeled, as would be expected for ~32 emitters within the point spread function of the objective. Even for emitters with randomly assigned fixed dipoles with respect to the microscope objective (blue), $M = 0.08$ for NT with 100% labeling.

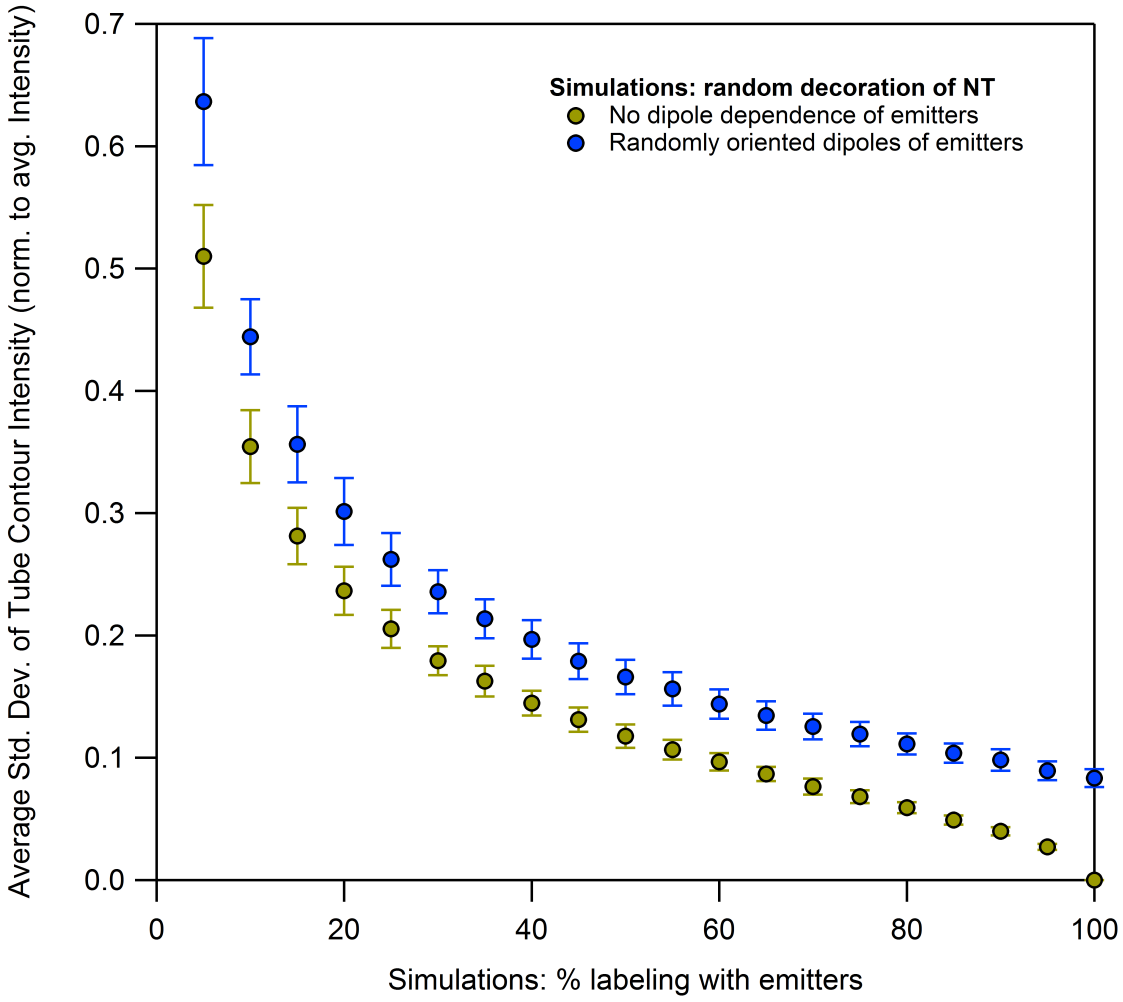

Figure S9: Simulated values for *M*, the average standard deviation of intensity along NT contours, normalized to average intensity, as a function of %-labeling with emissive decorating elements for two cases: NT with randomly placed decorating emitters, each having the same dipolar angle with respect to the microscope objective (yellow), and NT with randomly placed decorating elements, each having a random fixed dipolar angle with respect to the microscope objective (blue).

VIII. Microscopy of Ag_{14}-DNA-decorated NT

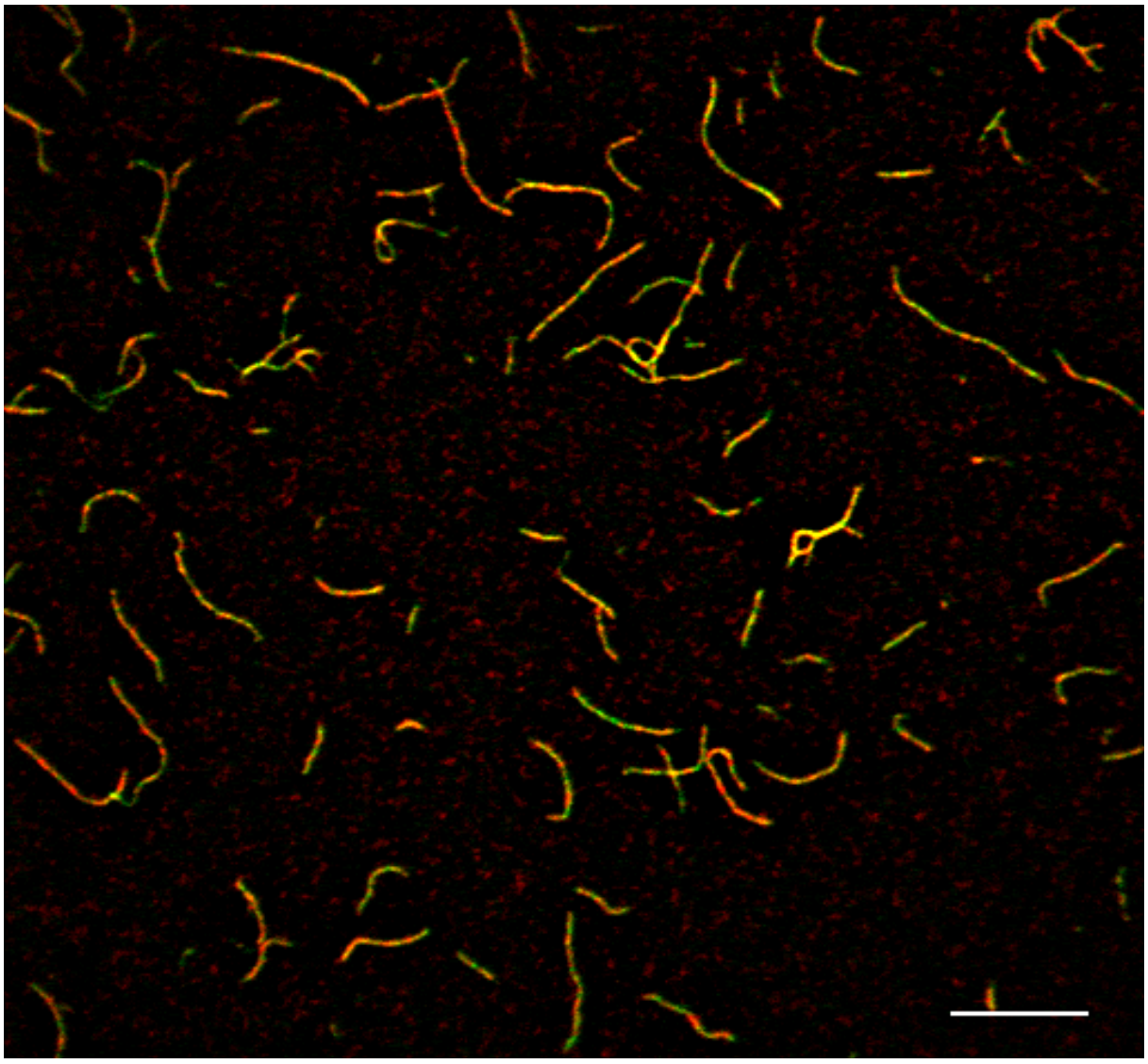

Figure S10: FAM-labeled NT decorated with Ag_{14} clusters. Overlap of confocal images of fluorescein-labeled NT with 100% U9 docking sites (green) decorated with purified Ag_{14}-DNA (red) after tube formation and embedded in PVA film on clean glass coverslips. Scale bar is 10 μm. Red and green fluorescence clear colocalize, indicating successful labeling of NT with Ag_{14}-DNA. (Intensities of red and green channels in overlap are adjusted to best illustrate each color to the eye and are not representative of actual intensities.)

IX. Individual Ag_{15}-DNA blinking on NT with 10% docker sites

Movie S1: Widefield microscopy image of 10H tubes, with 10% of U6 strands labeled with docking sites, decorated by Ag_{15}-DNA and embedded in PVA film. Widefield microscopy was used for imaging, as opposed to spinning disc confocal microscopy, to increase the intensity of light per each 1 second exposure window and therefore increase the probabilities of blinking and bleaching events. Three individual diffraction-limited spots, labeled 1, 2, and 3, are identified as single Ag_{15}-DNA by their "on-off" blinking and bleaching characteristics. The circle around each emitter changes from red, when the emitter is fluorescing, to blue, when the emitter is either bleached or in a long-lived dark state (a "blinking" state). Figure S10 shows intensity profiles for these three emitters.

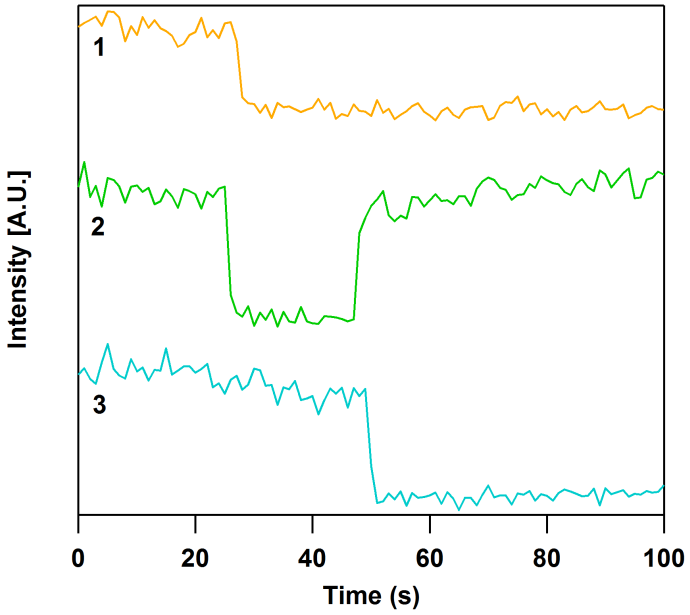

Figure S11: Intensity traces for three selected Ag_{15}-DNA emitters, as labeled in Movie S1. The intensity values plotted here are calculated by summing up all pixel values in a 7x7 pixel square, centered on each emitter. Each trace has two states: an "on" state marked by high intensity, and an "off" state marked by low intensity. The "off" states for all three traces have intensity values comparable to background noise – thus "off" states indicate that no fluorescent emitter is located within the 7x7 pixel square. Traces 1 and 3 show bleaching events for Ag_{15}-DNA, and trace 2 shows a blinking event, indicating that only one Ag_{15}-DNA is imaged at a time because the fluorescence states are binary.

X. Comparing *M* values for NT labeled with once-purified and twice-purified Ag_{15}-DNA

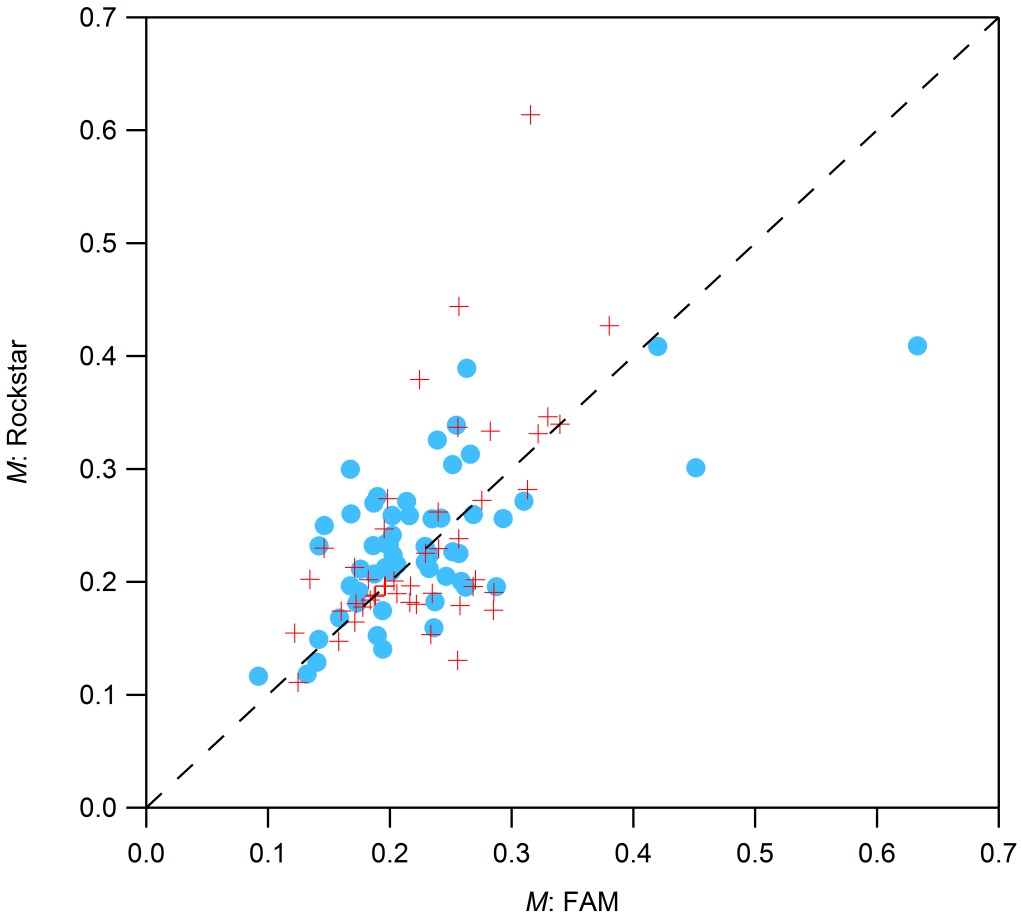

Figure S12: *M* values for NT labeled with once-purified and twice-purified Ag_{15}-DNA. *M*, the average standard deviation of the background-corrected intensity along each contour, normalized to the contour's average intensity, calculated for emission from FAM (x-axis) and from Ag_{15}-DNA (y-axis). NT have 100% U6 strands with dockers, FAM labels on U1 strands, and are labeled with red crosses for TEAA as the ion-pairing agent in the HPLC running buffer and with blue dots for purification with a second stage of HPLC using HFIP/TEA as the ion-pairing agent. The similarity between the distributions for NT decorated with clusters purified once and twice by HPLC indicates similar levels of purity in both cases. The second purification with HFIP/TEA was necessary for quantification of achieved purity by ESI-MS.

XI. References

(1) Yin, P.; Hariadi, R. F.; Sahu, S.; Choi, H. M. T.; Park, S. H.; Labean, T. H.; Reif, J. H. Programming DNA Tube Circumferences. *Science* **2008**, *321*, 824–826.

(2) Yeh, H.-C.; Sharma, J.; Han, J. J.; Martinez, J. S.; Werner, J. H. A DNA--Silver Nanocluster Probe That Fluoresces upon Hybridization. *Nano Lett.* **2010**, *10*, 3106–3110.

(3) Schultz, D.; Gardner, K.; Oemrawsingh, S. S. R.; Markešević, N.; Olsson, K.; Debord, M.; Bouwmeester, D.; Gwinn, E. Evidence for Rod-Shaped DNA-Stabilized Silver Nanocluster Emitters. *Adv. Mater.* **2013**, *25*, 2797–2803.

(4) Copp, S. M.; Schultz, D.; Swasey, S.; Pavlovich, J.; Debord, M.; Chiu, A.; Olsson, K.; Gwinn, E. Magic Numbers in DNA-Stabilized Fluorescent Silver Clusters Lead to Magic Colors. *J. Phys. Chem. Lett.* **2014**, *5*, 959–963.

(5) Copp, S. M.; Bogdanov, P.; Debord, M.; Singh, A.; Gwinn, E. Base Motif Recognition and Design of DNA Templates for Fluorescent Silver Clusters by Machine Learning. *Adv. Mater.* **2014**, *26*, 5839–5845.

(6) Wiggins, P. A.; van der Heijden, T.; Moreno-Herrero, F.; Spakowitz, A.; Phillips, R.; Widom, J.; Dekker, C.; Nelson, P. C. High Flexibility of DNA on Short Length Scales Probed by Atomic Force Microscopy. *Nat. Nanotechnol.* **2006**, *1*, 137–141.